DAMAGE OF WELDED STEEL STRUCTURES DUE TO STRONG EARTHQUAKES

by Kiyoshi KANETA[I] and Isao KOHZU[II]

SYNOPSIS

In order to examine actual cyclic inelastic behavior and fatigue strength of beam-column connections, flat and cross shaped butt-welded specimens were used to modelize beam, column flanges and diaphramns. Non-dimensional load-deflection relationship, energy absorption capacity concept and fatigue strength obtained from the experiment are discussed. And then, an experiment of cantilever beams consisted of wide flange sections under alternating bending was performed to verify load-deflection and moment-extreme fiber strain relationships and fatigue strength at or near the beam end, and to compare the results with another ones. These results are analytically expressed to compute the damage of steel structures.

INTRODUCTION

When a steel structure is subjected to destructive earthquakes, it may be possible to have low-cycle fatigue damage of the members or subassemblages due to repeated elasto-plastic deformations. The possibility that low-cycle fatigue damage may occur in critical components of a steel structure, depends mainly upon the strength, ductility and the energy absorption capacity of the structure, and intensities and durations of strong earthquake motions to which the structure would be subjected. In order to consider the former influence upon the low-cycle fatigue damage of such a structure, an experimental research is required to confirm cyclic inelastic deformation characteristics and low-cycle fatigue properties of structural steels, members and subassemblages. Attempts in order to clarify low-cycle fatigue properties of several structural steels, metals and alloys have been developed by many investigators in the past[1]. On the basis of these quantitative estimations, low-cycle fatigue damage of steel structures subjected to destructive earthquake motions has been computed numerically by several investigators[2]. In many investigations of the past, it has been considered that columns would have been mainly damaged during strong earthquake motions, but the possibility of the incremental collapse caused by so-called P-Δ effect is ignored. But, in design of general steel frames, most of these inelastic deformations should be confined to the girders because of safety and maintaining functional. Consequently, it is desirable to design steel structures as weak-beam, strong-column type, and to maintain the strains in column sections in the elastic range during earthquake excitations. In this case, there is a great deal of interest in the inelastic behaviors of the girders. When the girders are consisted of wide flange sections, it often happens that the girder flanges are connected with column flanges by means of butt welding and the girder webs bolted with the gusset plates welded to the column flanges, or connected to them by means of fillet or butt welding. It is reasonable that the cyclic load carrying and the inelastic deformation capacities at the location of the girder ends may be inferior to them at the original wide flange sections,

I Professor of Structural Engineering, Department of Architectural Engineering, Faculty of Engineering, Kyoto University, Sakyo-ku, Kyoto, Japan

II Research assistant, ditto

because of the reduction of the cross sectional areas caused by scallops which are necessary for security of welding performance, and the occurrence of heat hardening and residual stresses affected by welding.

In this point of view, the principal concept in this paper is focussed to the cyclic ductility and fatigue strength of welded beam-column connections.

EXPERIMENTAL PROCEDURE AND RESULTS OF TEST SERIES NO.1

Experimental procedure.- Specimens used in this test series, consisted of JIS SS41, 25 mm thick steel plates, were welded at right angles by means of CO_2-GAS butt welding or NON-GAS butt welding and fabricated to flat plate shapes which were named A-TYPE or crossed shapes named B or C-TYPE as shown in Figs.1 and 2, respectively. Selected combinations of welding procedures and specimen's types are tabulated in Table.1. Monotonic tension tests and cyclic tension-compression tests were carried out for three types of specimens at the longitudinal direction of them, but for only C-TYPE specimens, cyclic tests were conducted under a constant column flange axial loading in the range between 0.2 to 0.6 times of the yield flange force. Fig.3 illustrates a specified loading apparatus to supply the constant column axial force for C-TYPE specimens.

Every specimens in cyclic tests were repeatedly loaded with a constant distorsion amplitude in the elasto-plastic range between $\pm$ 0.5 to $\pm$ 1.5 % as the strains ($\pm$ 0.25 to $\pm$ 0.75 mm as the deformations) of the gauge length in a manner of quasi-static state, and controlled by a pair of electric extensometers located between the constant gauge length, 5.0 cm, as shown in Figs.1 and 2. An electronic universal testing machine (AUTOGRAPH) of capacity 50 tons was used to load specimens cyclically. Load was sensed by a transducer of tension-compression type mounted on the cross-head of the autograph, and recorded on an XY recorder together with distorsion amplitudes detected continuously by the foregoing electric extensometers. A number of strain gauges for measuring plastic strains were pasted on idealized, column flange sections, welded metal zones, diaphrams and girder flanges of all specimens, and then recorded by a digital printer of a multi channel strain-meter.

Experimental results.- Brittle fracture with a poor reduction of cross sectional area at column flange sections was observed for A-TYPE specimens in monotonic tension tests. Recorded strains at this section, at or near the fracture point, showed very lower values than those at the rolled direction of the base metal. On the other side, B-TYPE specimens fractured ductile at the sections far away from mid points of specimens.

Stability of the hysteresis loops is much remarkable during almost overall cycles except the initial and final states. These loops at the steady states are named cyclic load-deflection ones and typical examples are shown in Figs.4~6, about three types of specimens and together with the base metal's.

Considerations of the results

a) Cyclic load-deflection relationship:

As it is clear from Figs.4~6, we can conclude that hysteresis loops have good stabilities and any significant difference is scarcely observed

from shapes of specimens and welding procedures. Fig.7 is a plot of the relationship between the non-dimensional peak load, P/Pp, (P: the peak load and Pp: the proportional limit load) and the non-dimensional distortion amplitude, $\delta/\delta p$, (δ: the selected distortion amplitude, and δp: the proportional limit amplitude in the initial state) in the steady state except C-TYPE specimens. By using the least squares method, we can approximate this relation to a bi-linear curve, and the following formula is obtained.

$$|P/Pp| = 0.041 \cdot |\delta/\delta p| + 1.1 \qquad (1)$$

And this formula is lined straightly in Fig.7.

b) Cyclic energy dissipation:

Because of the importance of the amount of energy absorbed and dissipated for the dynamic response of a structure in the event of earthquakes, it is much of interest to know the evaluation of the cyclic energy dissipation of the welded joints. Popov et al.[3] have suggested this relationship in terms of dimensionless permanent deflection ratio and the energy ratio based on the energy dissipated during a single excursion in the ordinary axis, and the former is named πd and the later named $e(=2W/Pp \cdot \Delta p)$. But, in the previous result of the writers' investigation, it has been noted that a linear relationship in the log-log scale diagram, with a good agreement, can be observed between the plastic strain amplitude and the energy dissipated per cycle[4]. Therefore, also in this investigation, as illustrated in Fig.8, the plot was made on a log-log scale and the least squares approximation is attempted. The empirical formula can be obtained as follows with the close correlation.

$$e = 1.55 \cdot \pi d^{\frac{1}{1.17}} \qquad (2)$$

c) Bi-linear approximation for the cyclic load-deflection relationship:

It is well known and has been reported by many investigators in the past that the cyclic load-deflection curves can be well fitted accurately using Ramberg-Osgood functions and by employing Masing's hypotheses. However, such functions are not convenient for a damage analysis even though rapid progress of digital computers in the recent years could lessen the complication of this calculation. Then, in this investigation, an attempt to make hysteresis curves bi-linear approximation is done. Emphasis is placed on the fact that the area enclosed by a bi-linear loop is equal to that of the experimental hysteresis curve. This view-point is much meaningful for the discussion of energy absorption concept during earthquakes in dynamic analysis. Namely, using Eqs.(1) and (2), the process is derived herein to assign definite values to the secondary branch on the bi-linear hysteresis loop, as shown in Fig.9.
Then

$$-\delta a/\delta p = e/[(1-\alpha) - \beta] - \mu \qquad (3)$$

$$Pa/Pp = e/[(1-\alpha) - \beta] - (\alpha\mu + \beta) \qquad (4)$$

where e: non-dimensional absorbed energy per half cycle,
μ: $= \delta/\delta p$, the ductility factor,
α, β: coefficient and constant of Eq.(1), and
$-\delta a$, Pa: co-ordinates of the secondary branch on the upper side.
Another co-ordinates are symmetric with respect to the or-

igin.

Experimental hysteresis curves and bi-linear approximated ones solved by use of Eqs.(3) and (4) are shown in Fig.10. The comparison with experimental results is quite satisfactory.

d) Estimation of low-cycle fatigue strength:

The non-dimensional plastic strain range, πd, which can be derived by deviding plastic distortion ranges by gauge length, 50 mm, and the number of cycles, N_f, at which the specimen is broken, were plotted and shown in Fig.11. By the least squares method, the following equation is obtained.

$$\pi d = 149 \cdot N_f^{-0.53} \qquad (5)$$

EXPERIMENTAL PROCEDURE AND RESULTS OF TEST SERIES NO.2

Experimental procedure.- In order to determine cyclic behavior and fatigue strength of more actual welded connections used in construction of steel buildings in Japan, this experiment was carried out. Specimens such as shown in Fig.12 were designed similar those employed by Popov et al.(3), because of the easy comparison with test results. In all of these specimens, the cantilever beams and columns were consisted of JIS SS41 wide flange sections. Connections of beam to column were all welded, namely, the flanges of the beams were welded to those of the column stubs by means of full penetration welding with backing metal or backing weld, the webs of the formers were welded to the later's stubs by means of fillet welding and each fillet of the beams at the connections was cut semi-circularly before welding. Column stubs of specimens were securely bolted with a rigid reaction beam and a double-acting hydraulic jack of capacity of 10 tons and a transducer were attached with a reaction column by PC-bars (high tensile strength steel bars) and pinned with the tip of the specimen, and then an electric extensometer was placed on the opposite side of the loading apparatus. Moreover, a guide frame to prevent lateral buckling was erected. The general arrangement of the equipment may be seen in Fig.13.

Cyclic loads with a constant distortion amplitude were applied in a quasi-static manner, these continuous relationships were recorded by an XY recorder. In order to examine the behavior of the plastic strains of the beam flange at the column face, many plastic strain gauges were pasted and measured in the same manner of test series No.1. In every experiment with cyclic load sequence, the work was terminated only after an actual failure of the beam flange had occurred.

Experimental results.- Several hysteresis loops of selected distortion amplitudes are reproduced in Fig.14. In general, hysteresis loops can be stabilized after a few cycles at the beginning and maintained to the number of almost 70~80 % cycles to the failure, although only a local-buckling could happen at the beam flange in the compression side, at higher distortion amplitudes. Selected distortion amplitudes and the number of cycles to failures are tabulated in Table.2.

Considerations of the results

a) Cyclic moment-extreme fiber strain relationship:

Dividing the peak moment, M, or the extreme fiber strain, ε, by each plastic value, Mp, or εp respectively, the dimensionless approximation has

been attempted by using strain outputs. The skeleton curve can be drawn in Fig.15, and the formulation is as follows.

$$|M/Mp| = 0.044 \cdot |\varepsilon/\varepsilon p| + 1.0 \qquad (6)$$

It can be noted that the constant and the coefficient in Eq.(1) are good agreement with those in Eq.(6).

b) Estimation of cyclic load and tip deflection relationship:
Generally, the elastic tip deflection is expressed as follows,

$$\delta = \delta_b + \delta_s \qquad (7)$$

where δ: the total tip deflection,
δ_b: the tip deflection due to the bending moment, and the value is divided into the deflection contributed by the elastic rotation at the location of the scallop and that by the rotation of the original wide flange section. And
δ_s: the tip deflection due to the shear force.

But, in the inelastic range, this relation becomes somewhat complicated, especially on the occasion of cyclic loading. In order to simplify this calculation, Popov et al.[3] have suggested the approximated, moment and the average curvature of the beam end relationship. As the strain or the curvature of the beam end is the most important value for the fatigue damage analysis because of the existence of the scallop, the writers induced another approximate relations between the curvature and the tip deflection after referring the paper[3].
Then

$$\delta = \delta_e + \delta_s + \delta_{p1} + \delta_{p2} \qquad (8)$$

where δ_e: the elastic tip deflection,
δ_s: the tip deflection due to the shear force,
δ_{p1}: the tip deflection contributed by the plastic rotation at the location of the scallop, and
δ_{p2}: the tip deflection by the plastic rotation of the original wide flange section.

δ_{p1} and δ_{p2} can be derived from the average curvature, ϕ_{av}, between both ends of each section, Δl, and the length from the end to the tip.
Namely,

$$\phi_{av} = (\phi_a + \phi_b)/2 \qquad (9)$$

$$\delta_{p1} \text{ or } \delta_{p2} = \phi_{av} \cdot \Delta l \cdot (l - \Delta l) \qquad (10)$$

where ϕ_a, ϕ_b: the curvature at the end of each section, $\geq \phi_p$.

By using Eqs.(2) and (8)$\sim$(10), the skeleton curve is appriximated with a good accuracy. Besides, using modified formulae of Eqs.(3) and (4) to the non-dimensional moment-curvature relationship, the hysteresis curves of load-tip deflection relationship can be drawn as the dashed ones in Fig.14. The experimental hysteresis curves can well be approximated by the predicted ones.

c) Estimation of low-cycle fatigue strength:

The non-dimensional cyclic plastic strain range, πd, at the beam end and the number of cycles to failure, Nf, are plotted as Fig.16. In the same manner of test series No.1, the following equation can be derived.

$$\pi d = 103 \cdot Nf^{-0.57} \qquad (11)$$

GENERAL CONCLUSIONS

From the results of both test series, the following conclusions may be drawn:

1) Cyclic load-deflection relationship can be derived approximately by using the bi-linear skeleton curve and the energy dissipation concept per half cycle of loading.

2) Within the scope of this experiment, the effect of column axial force is little significant to the fatigue strength and the energy absorbing capacity of the girder.

3) It may be considered that there is no effect of difference in welding procedures and bevel angles on the fatigue strength in a constant distortion amplitude.

4) But, it can be observed that fatigue strength deteriorates a little owing to the stress-concentration caused by scallop.

REFERENCES

[1] for example, Morrow, J., "Cyclic Plastic Strain Energy and Fatigue of Metals", INTERNAL FRICTION, DAMPING, AND CYCLIC PLASTICITY ASTM STP 378, 1964, pp.45 - 87.

[2] for example, Kajiraj, I. and Yao, J.T.P., "Fatigue Damage in Seismic Structures", J. Structural Division, ASCE, Vol. 95, No. ST8, Aug. 1969, pp.1673 - 1692.

[3] Popov, E.P. and Bertero, V.V., "Cyclic Loading of Steel Beams and Connections", J. Structural Division, ASCE, Vol. 99, No. ST8, June 1973, pp.1189 - 1204.

[4] Kaneta, K., Takeguchi, K. and Kohzu, I., "On the Strength and Ductility of Welded Joints Subjected to Low-Cycle Elasto-Plastic Deformations", Proc. of the Third Japan Earthquake Engineering Symposium-1970, pp.667 - 674.

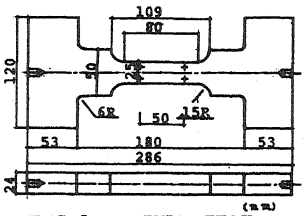

FIG.1: A-TYPE TEST SPECIMEN

welding process	TEST SPECIMEN		
	A	B	C
CO2-GAS	$\bar{L}$,I,L,	I,L	I,L
NO -GAS	L		

$\bar{L}$: single bevel butt weld with backing weld
I: square butt weld with backing metal
L: single bevel butt weld with backing metal

core wire: CO_2-GAS:MG50
NON-GAS:OW56

TABLE.1: WELDING PROCESSES AND GROOVES

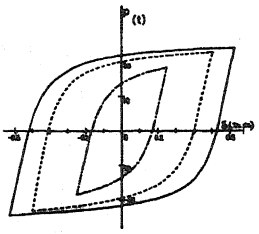

FIG.5: HYSTERESIS LOOPS OF B-TYPE TEST SPECIMENS

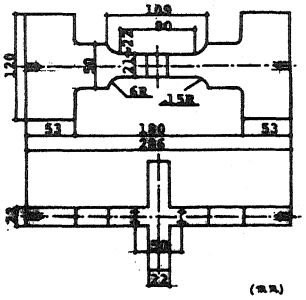

FIG.2: B&C-TYPE TEST SPECIMEN

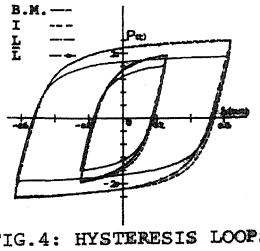

FIG.4: HYSTERESIS LOOPS OF A-TYPE TEST SPECIMENS AND BASE METALS

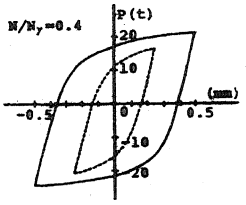

FIG.6: HYSTERESIS LOOPS OF C-TYPE TEST SPECIMENS

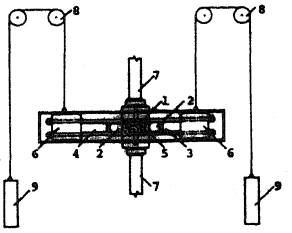

1: specimen
2: pin joint
3: hydraulic jack
4: transducer
5: PC bar
6: rigid beam
7: pull rod (AUTOGRAPH)
8: pulley
9: counter-weight

FIG.3: LOADING APPARATUS FOR C-TYPE TEST SPECIMENS

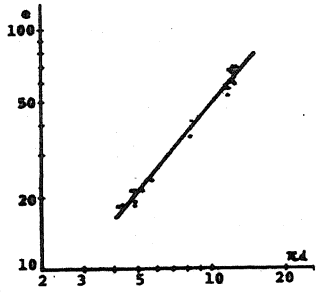

FIG.8: e-πd RELATION OF TEST SERIES NO.1

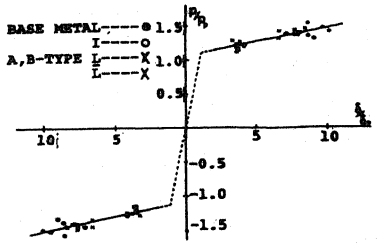

FIG.7: BI-LINEAR APPROXIMATION OF THE SKELETON CURVE (SERIES NO.1)

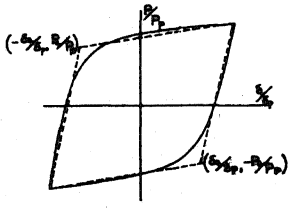

FIG.9: BI-LINEAR MODEL OF HYSTERESIS LOOP

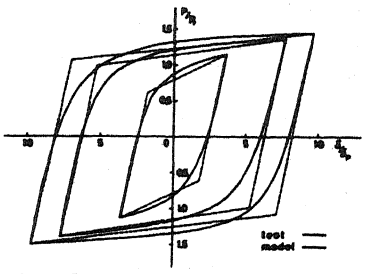

FIG.10: EXAMPLES OF BI-LINEAR MODELS FOR TEST SERIES NO.1

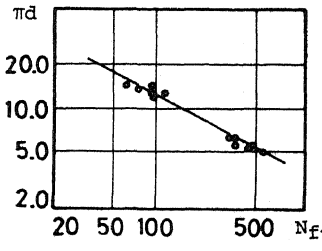

FIG.11: πd-N_f RELATION OF TEST SERIES NO.1

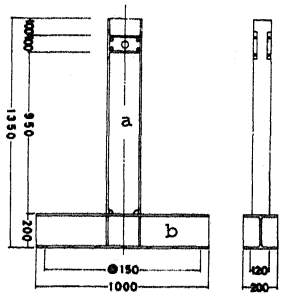

FIG.12: CANTILEVER a: H-200×100×5.5×8
SPECIMEN b: H-200×200×8×12

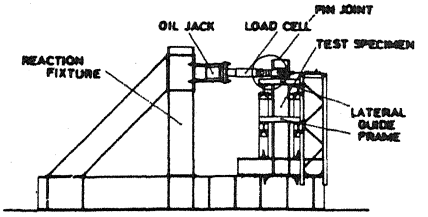

FIG.13: GENERAL ARRANGEMENT OF TEST SERIES NO.2

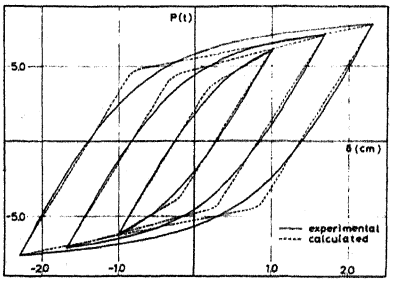

FIG.14: HYSTERESIS LOOPS OF TEST SERIES NO.2

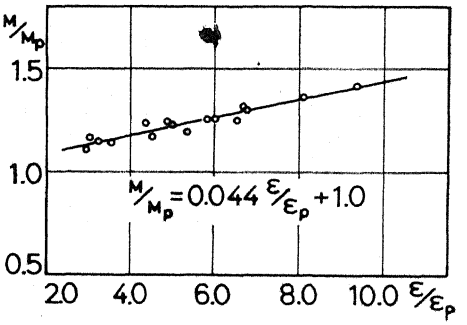

FIG.15: BI-LINEAR APPROXIMATION OF THE SKELETON CURVE (SERIES NO.2)

DISTORTION AMP., δ(cm)	1.00	1.26	1.52	1.68	1.78	2.30
N_f (CYCLES)	135 189 *211	53 *94 *127	*54	32	*39	16

*: SPECIMENS WITH BACKING WELD

TABLE.2: THE RESULTS OF TEST SERIES NO.2

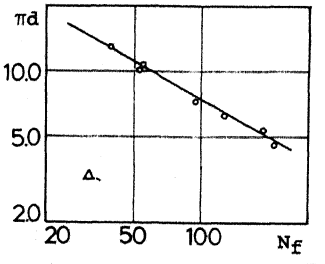

FIG.16: πd-N_f RELATION OF TEST SERIES NO.2